Development of new pervaporation composite membranes for desalination: Theoretical and experimental investigations

Tarik Eljaddi, Deisy Lizeth Mejia Mendez, Eric Favre, Denis Roizard

Development of new pervaporation composite membranes for desalination: theoretical and experimental investigations [1]

Tarik Eljaddi, Deisy Lizeth Mejia Mendez, Eric Favre, Denis Roizard*

Université de Lorraine, CNRS, LRGP, 1 rue Grandville, F-54000 Nancy, France

* Corresponding author: Denis Roizard

Abstract

Pervaporation (PV) has mainly been used for dehydration in industrial applications as well as for the recovery of some organic components from various organic or water mixtures. Nevertheless, to date, pervaporation has never been seen as a potential industrial solution to get drinkable water by water permeation, contrarily to membrane distillation (MD). Nevertheless, at the lab scale, some studies with hydrophilic PV membranes have been reported. This work intends to underline the potential industrial interest of hydrophobic PV composite membranes for desalination. Indeed, even in hypersaline solutions, the water activity remains very high (>0.9), and it is wise to use membranes with stable properties in water to guarantee steady performance. Therefore, this study investigates the interest of hydrophobic polymers as coating selective layers for desalination. To guide our choice, a rational approach was used based on the prediction of the membrane resistance to water transfer. Polymethylpentene, poly(1-trimethylsilyl-1-propyne) and Teflon AF2400 were tested as the top layer to obtain hydrophobic composite PV membranes. Several feed NaCl solutions with or without a surfactant were used to investigate the mass transfer properties of these PV membranes for water treatment comparatively to more conventional porous membranes (e.g. PVDF) currently studied in membrane distillation.

Keywords:

pervaporation, hydrophobic selective layers, resistance in series model, wetting issue, desalination

[1] This work has been partly presented as an oral communication at Euromembrane 2018 (Valencia)

1. Introduction

Today, more than 663 million people live without access to drinkable water and 1.8 billion people relying on fecal-contaminated water [1]. Moreover, after its use by man, the quality of water is usually altered, either physically, e.g. temperature increase, or by anthropic pollutants. Water that can be used directly corresponds only to 0.6% of the total water, which is why worldwide water reclaiming technologies are the focus of incentive policies. The main source of easily available large amounts of water is salted water. Hence, improving desalting technologies is of upmost importance.

At the industrial scale, there are two main types of desalination processes, either thermal processes based on distillation technologies, e.g., multistage flash (MSF) [2], multi-effect distillation (MED) [3], or mechanical processes using membrane processes, i.e., reverse osmosis (RO). Distillation is the traditional technology, but RO, lately developed in the 1970s, is now mainly used. RO corresponds to more than 65% of the total world installed capacity [4], and the total water cost for 1 m^3 is 0.5-1.2 US$ for sea water RO and 0.2-0.4US$ for brackish water RO, while the cost is between 0.7 and 1.5 US$ for MSF and MED [5]. Electrodialysis (ED) can also be used for wastewater and brackish water, especially to concentrate nutrients, such as potassium, nitrogen and phosphate, under similar conditions; the cost of ED is similar to the cost of RO, but ED is not as flexible as RO, and it requires several stages to reach the same industrial target, which means higher capital cost expenditures.

Other membrane technologies can be used for water desalination, such as forward osmosis (FO)[6], pervaporation (PV)[7] or membrane distillation (MD)[8]. To date, these last three technologies and related membranes have been less mature and less attractive from an energetic viewpoint for desalination applications. For instance, with FO, the regeneration cycle of the pristine draw solution must be achieved by another technology, possibly by RO. On the other hand, MD and PV are both thermal processes where the water is transferred through the membrane as vapor, thus giving rise to a higher energy demand.

Many reviews have already been published on water desalting using various membrane technologies. Most of them make use of polymeric membranes, but some works also report the use of inorganic membranes [9]. Quite recently, the electrospinning method has also become a new approach to obtain MD membranes made of nanofibrous materials [10,11]. As far as polymeric membranes are concerned, these reviews present several key parameters, i.e.,

energy efficiency and the possible use of low grade energy [12–14], pore wetting and hydrophobic modification to limit the flux decay and increase the time life of the membranes [13–16], and fouling resistance linked to organic matter [17,18].

Several strategies have been developed to tackle the wetting issue arising in MD. Notably, surface engineering by chemical functionalization, such as plasma modification and grafting [16], and physical modifications [15] of the top layer to enhance the hydrophobic properties of the pores have been established and hence prevent the usual wetting trend of the porous top layer. Additionally, anti-wetting membranes have been designed thanks to the stabilization of the liquid-vapor interface at the mouth of the pores. With the same objective, various types of nanoparticles have also been used to tailor the omniphobic properties of the pores, e.g., by the incorporation of multiwalled carbon nanotubes, nanosized SiO_2 and TiO_2 particles into polymeric membranes (e.g., porous polyvinyldifluoride (PVDF) membranes), resulting in a significant increase in the contact angles (> 150°) [13].

In the 1990s, the design of membranes that can avoid the penetration of liquid water has already been studied by several research groups, specifically by coating porous membranes to generate a dense top layer able to fully eliminate any wetting hazard [19,20]. The three main issues of this approach are to avoid pore plugging, to control the permeance of the dense top layer and to obtain good adhesion between the top layer and the porous layer. It must be emphasized that the introduction of this dense top layer gives a composite pervaporation membrane. Thus the water transfer occurs according to the solution-diffusion mechanism [21]. This approach was proven to be efficient for obtaining pure water vapor from various feeds, such as fruit juice [22] or hypersaline effluents [23]. In this last case, using uncharged, dense hydrophobic membranes, the salts dissolved in the feed have extremely low sorption coefficient in the dense polymeric layer; moreover the salts would not be vaporized from the downstream side of the coating layer. More examples can be found in the reviews of Wang (2016) and Zhong (2020) [7,24].

Pervaporation involves a thermodynamic change from the feed side (liquid phase) to the permeate side (vapor phase) and the mass transfer is induced by the difference between the partial pressures established between the upstream and downstream sides of the membrane. Several operating conditions can be used to fix the require partial pressures. Interestingly, pervaporation can be operated at atmospheric pressure using a lower temperature range

compare to distillation. When a lower temperature is applied at the downstream side under atmospheric pressure, these conditions named “thermo-pervaporation” create the activity difference through the membrane which induces the mass transfer. Hence low-grade energy can be used to run the process, which is similar in the direct contact membrane distillation (DCMD). Thus it should be noted that using a temperature difference to treat hypersaline effluents is very favorable from energy viewpoint compared to RO and could give rise to new hybrid processes [25]. Thermo-pervaporation has been known for years [26,27] but yet never applied in industry; nevertheless when a temperature difference can easily been applied to generate a vapor pressure difference across the membrane, the mass transfer from the upstream side to the downstream side occurs like with the conventional vacuum driven pervaporation. However, one parameter can be different: it is the state of the downstream side of the membrane which might be more swollen than when vacuum is applied. In the case of hypersaline water solutions, this difference is not a drawback and does not alter the selectivity of the process because water is the only volatile component of the mixture.

As stated from the literature review given above [7,24], the coating layers used to obtain PV membranes useful for desalination were prepared with strongly hydrophilic polymers, such as sulfonated polyethylene, quaternized polyethylene[19], alginic acid-silica hydrogel coatings [28, 29], chitosan [30], polyelectrolyte polymer (Nafion type)[31], cellulose [23] or polyvinyl alcohol [32,33].

As the objective of the separation is to transfer water, this choice of using very hydrophilic coatings appears to be quite logical and related to the solution-diffusion mechanism of PV. Nevertheless, sorption is not the only parameter that governs PV selectivity. In addition, there is a major difference between the use of a PV membrane to dehydrate an azeotropic mixture or to achieve desalination. Indeed, in the first case, water is the minor component, whereas in the second case, water is the main component. Hence, as the activity of the water in the feed is much higher in the second case, above 0.9 [34], the best membranes used for azeotrope splitting are certainly not the ones that would be the best for desalination for two reasons: a) the conventional dehydrating PV membrane might be unstable at such a high water activity and may be damaged while contacting the saline water solutions, and b) as the hydrophilic top layer is often crosslinked, the sorption phenomena will be blocked to a large extent.

Therefore, in this work, we investigated the use of specific nonpolar polymers, mainly hydrophobic polymers, which have never been considered to develop composite PV

membranes useful for water treatment. To select appropriate polymers and to guide our choice, we use a rational approach based on their permeance for water. Several PV membranes were prepared and tested using a direct contacting cell. As there is only a small difference in water activity between brackish water and hypersaline solutions, as a RO retentate, synthetic NaCl solutions up to 10g/L were used with and without a surfactant to determine the flux and the rejection rate.

2. Experimental

2.1. Reagents

The pristine support used in this study is porous PVDF (Durapore™, filter GVHP, pore size 0.22 µm, porosity 75%, thickness: 122 µm), obtained from Merck Millipore. The polymers used to build dense top layer on the PVDF support are polymethylpentene (PMP) and poly(1-trimethylsilyl-1-propyne) (PTMSP) obtained from Sigma-Aldrich, and copolymers of poly(2,2-bis(trifluoromethyl)-4,5-difluoro -1,3 dioxole-cotetrafluoroethylene) (TeflonAF®2400, DuPont) (**Figure 1**). The organic solvents used to prepare polymer solutions are cyclohexane (Sigma-Aldrich) and Fluorinert FC75™ (3M). Ultra-pure deionized water (Milli-Q) was used to prepare all the aqueous solutions (conductivity <3 µS), NaCl was used to prepare the salted solutions, and the surfactant sodium dodecyl sulfate (SDS) was obtained from Sigma-Aldrich.

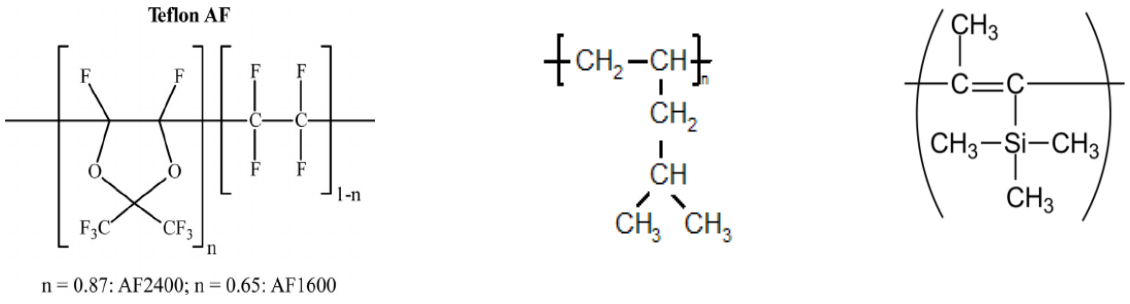

Figure 1: Structure of polymers: Teflon AF2400, PMP and PTMSP

2.2. Composite membrane preparation

The first step was the preparation of the polymer solution, with the dissolution of the polymer mass in cyclohexane (PMP: 2 wt% and PTMSP: 2wt%) or in Fluorinert FC 75TM (Teflon

AF: 1 wt%) to obtain homogenous solutions. In the second step, an ultrasonic bath was used to eliminate the air bubbles, and then the applicator film (Elcometer 4340 Motorized Film Applicator) was used to cast the polymer solutions on the surface of the PVDF support. After the evaporation of the solvent, the composite membranes were dried for several days before characterization and utilization.

2.3. Characterization methods

The prepared membranes were characterized by infrared spectroscopy (IR) (BRUKER, ALPHA-P in attenuated total reflection (ATR mode), scanning electron microscopy (JEOL, JSM 649V) and contact angle measurements.

The adhesion tests were performed with the Elcometer 510 Pull-Off Adhesion Gauge; this automatic gauge and Locite-Snellijmen Glue were used. Pristine and composite membranes were tested three times and the average value is reported. The observed mean deviation was small, about ±1%.

The conductivity measurements were performed with the bench conductivity meter Jenway 4520, purchased with glass a conductivity probe with ATC (K= 1/cm).

More details on characterization methods can be found in supplementary data " Data in Brief".

2.4. Characterization of the water mass transfer in a direct contact membrane setup

The same apparatus was used to characterize the water transfer through the porous PVDF membrane, i.e. by membrane distillation process, and through the dense PV membranes, i.e. by thermo-pervaporation). The performance of the pristine PVDF and of the three composite hydrophobic membranes (top layer: PMP, PTMSP, AF2400) were determined thanks to a direct contact membrane configuration having an active surface of 40 cm^2 (**Figure** 2; see also **Figure** 1S, Supplementary material section). The centrifuge pumps, temperature sensors, and flux sensors were purchased from RS Components, and the balance was acquired from Sartorius (0.01 g).

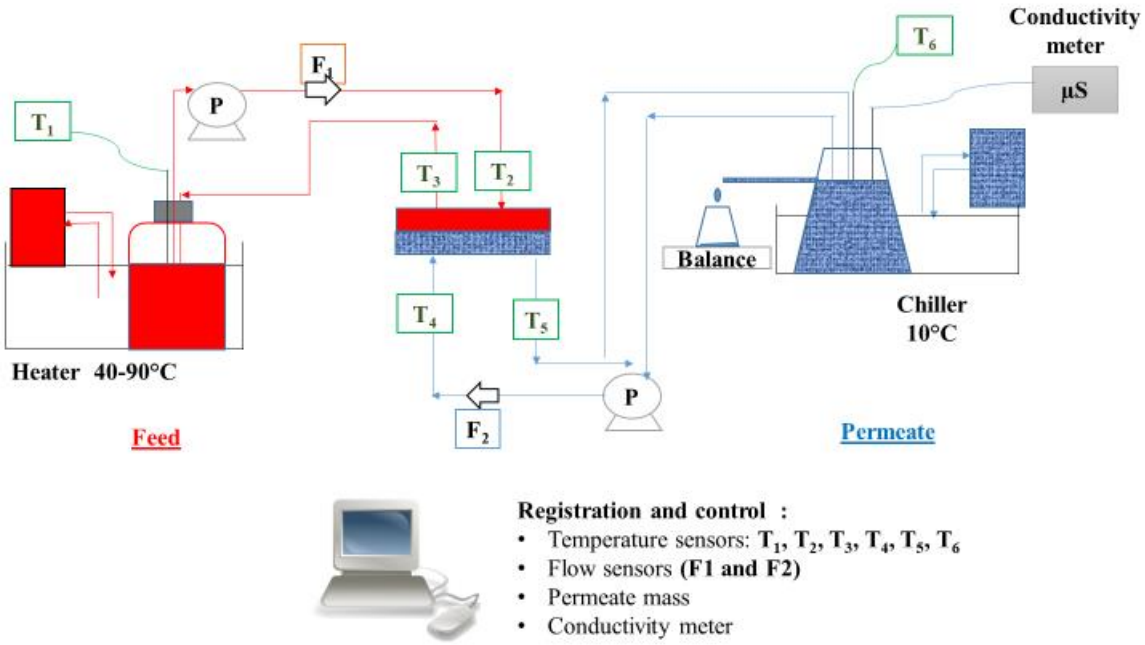

Figure 2: General scheme of the direct contact membrane (DCM) setup.

Operating conditions: both the feed and the permeate solutions were circulated in closed loops and the cross flow was ensured on each side of the membrane. The applied flow rates were 1 L/min on the feed side and 0.8 L/min on the permeate side. The water vapor was condensed on the permeate cold side and the obtained liquid water in excess was continuously weighed online with a balance. The conductivity of the 3 g/L and 10 g/L feed solutions were 6.5 and 18.9 mS/cm, respectively, at room temperature. At the permeate-side, the measured water conductivity was close to zero and the measurements are given in µS/cm.

For each experiment, the feed solution, initially pure water on the feed side, was circulated for approximately 2 h to reach steady state conditions linked to the stabilization of temperatures on both sides of the membrane. The warm and cold temperatures were controlled at the inputs and outputs of the cell. All these data were registered on a computer via the software LabVIEW.

The water vapor that permeates through the membrane was condensed on the downstream side in the flowing cold liquid. The excess liquid was directly collected and weighed. The steady state was obtained approximately after 1 hour thanks to the temperature regulations of the feed and permeate reservoirs connected to the cell. Under steady-state conditions, the water mass increase in the permeate side was linear versus time. Measurement accuracy is about 5% (**Figure** 2S, Supplementary material section).

3. Results and discussion

3.1. Advantage of PV and MD to treat high salinity solutions

If reverse osmoses is currently the benchmark technology to obtain drinking water from seawater, then the situation rapidly changes when the salt concentration increases because the energy demand rises very rapidly. This is the case for the brine generated by RO, whose salt concentration can increase up to 120 gL^{-1}. Indeed, relatively to seawater, the osmotic pressure at 40°C is dramatically increased by a factor of 250, as calculated from the van 't Hoff equation (**Figure** 3). However, for other technologies, such as PV and MD, the main driving force is the water partial pressure and not the osmotic pressure. Thus, it is interesting to calculate the variation in the water partial pressure with increasing salt concentration. Considering brine as the salted feed, it can be shown that there is also a decrease in the water partial pressure. However, it can be seen in **Figure** 3 that the pressure decrease is in fact very limited, i.e., only of a factor of 1.031 compared to seawater at the same temperature. That is why for PV and MD technologies, the energy demand does not vary significantly with the salt concentration, while for RO, the energy demand becomes extremely high. Hence, clearly, the salt concentration for PV and MD is not a thermodynamic barrier, and more water could be extracted by water vaporization even from brine.

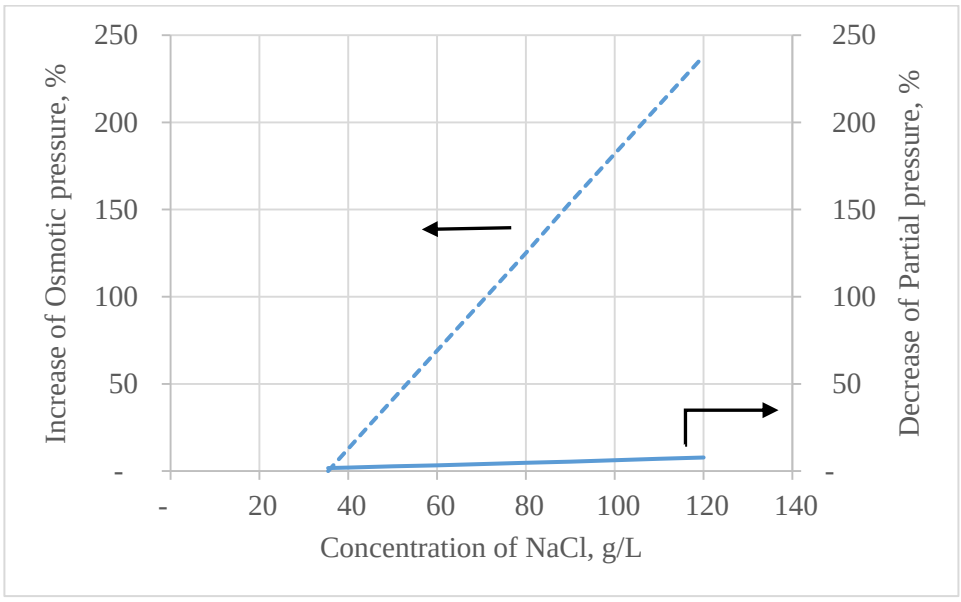

Figure 3: Effect of the NaCl concentration on the osmotic pressure (dashed line) and on the water partial pressure (solid line). NB: sea water is approximately 35.5 g. L^{-1}, while RO brine is ≈120 g. L^{-1}. Taking the sea water as the reference point for the brine at 40°C, the osmotic pressure is increased up to 106 bar, while the water pressure vapor is only reduced from ≈73 497 to 67 747 Pa (-7%). Data are from [35,36].

MD initially appeared to be the most promising technology to improve water desalination, especially because of its high productivity, but after two decades of extensive research, the major issue of wetting has not yet been solved. In fact, the wetting issue has led to a much lower productivity than expected of MD using porous membranes and to extra operational costs to dry and recondition the membranes. Therefore, it was our aim within this work to investigate to what extent PV membranes could effectively be applied to desalination. Indeed, pervaporation is used conventionally to extract the minor component of a feed whereas in desalination, water is the major component to be extracted. Thus the membrane must be enough stable at high water activity and the flux must be high enough to satisfy industrial criteria. We carried out this study following two steps:

- To find a way to predict the productivity of PV membranes to clarify their potential industrial interest and to create a tool to design appropriate membranes.
- To achieve the preparation of some original membranes to test their performance with some model solutions, in comparison to the prediction and to the MD membranes.

3.2. Selection of the polymers and an evaluation of the potential properties

Industrial membranes are composite membranes gathering several layers, each of which is chosen to bring a specific property, such as the selectivity, mechanical resistance or even a gutter layer [37]. Regardless of the type of separation, the mass transfer coefficient ($k_{composite}$) is linked to the resistance of the composite membrane ($R_{composite}$), which is known to follow the resistance-in-series model [38]:

$$\frac{1}{k_{composite}} = \frac{1}{k_{layer\,\#1}} + \frac{1}{k_{layer\,\#2}} + \cdots \qquad \text{Equation (1)}$$

with $R_{composite} = 1/k_{composite}$

Thus, this simple equation can be used to predict the mass transfer through a composite membrane. A qualitative description of the transfer is given in **Figure** 4. In the case of a PV desalination membrane, the composite membrane must have a minimum of two layers, i.e., a dense layer-coated on a porous mechanical support.

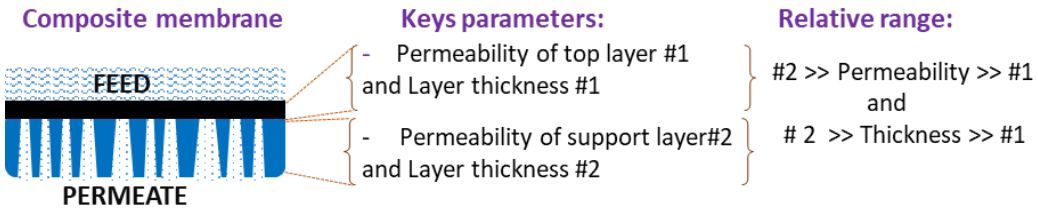

Figure 4: Mass transfer parameters governing the permeance of a composite membrane

Thus, the global mass transfer $k_{composite}$ ($m.s^{-1}$) can be calculated by equations 1 and 2 [39]:

$$k_{dense}=\frac{P.R.T}{e_{dense}} \quad \text{and} \quad k_{porous}=\frac{D.\varepsilon}{\tau.e_{porous}} \qquad \text{Equation (2)}$$

where k_{dense} is the mass transfer of the dense layer that is a function of its permeability P and of R the ideal gas constant (in J/mol. K in the international system of units, T is the temperature (K), e_{dense} is the thickness of the dense layer (m) and k_{porous} is the mass transfer of the porous support. This parameter is a function of the diffusion coefficient (D) (m^2/s), ε is the porosity, τ is the tortuosity and e_{porous} is the thickness of the porous support. In the international system, the permeability is expressed in ($mol.m.m^{-2}.Pa^{-1}.s^{-1}$) but more usual unit in membrane distillation is in $kg.m.m^{-2}.s^{-1}.bar^{-1}$.

The literature permeability data taken for the dense polymer layers are gathered in the supplementary Table 1S. Obviously, the dense polymers have a lower permeability than the porous PVDF. That is why the thickness of the dense layers must be as low as possible to minimize the overall resistance of the composite membranes. At the industrial level, the thickness of the selective layer is in the range of 0.1 to a few micrometers [40]. Recent papers have shown that much thinner dense layers can be prepared, with thicknesses down to ≈10 nanometers [41]. This means that the permeance (Pe) of a dense layer, defined as the ratio of the permeability to the thickness, can nevertheless reach a high value despite the dense structure of the layer.

The mass transfer coefficients of the porous and dense skin layers of the polymers used were calculated for H_2O by equation (2). The relationship between the mass transfer coefficient and the thickness is shown in **Figure 5** for various types of polymers:

- porous PVDF (a typical membrane used for MD),

- PMP, PTMSP, and Teflon AF 2400 (three glassy polymers used as dense coating layers, known for their high free volume content (≈28-30%)). Note that PTMSP is known to suffer from aging effect affecting its free volume and its permeability.

Considering the average thickness of the porous membranes used in MD of 200 µm, **Figure 5** clearly shows that PTMSP, AF2400 and even PMP can reach the same range of the mass transfer coefficients if the thickness of the active layer is in the range 0.1-1 µm. As thin layers cannot be used as self-standing membranes, they need to be used as composite membranes, for instance, by deposition on a porous support layer. Hence, using porous PVDF membrane distillation as a support (≈ 200 µm) would theoretically provide a composite membrane with a mass transfer coefficient that can be predicted by equations 1 and 2. In fact, some deviations from the theoretical calculation can occur due to the experimental preparation that may induce some known defects, such as the nonhomogeneous thickness of the-coated layer and some pore plugging of the support membrane. Of course, any pinhole defect must be strictly avoided.

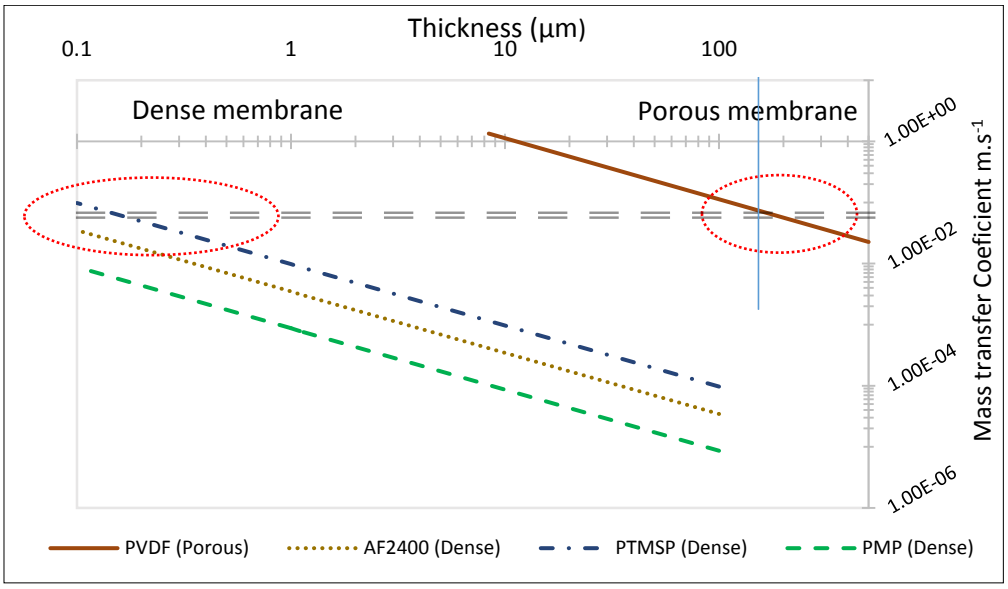

Figure 5: Prediction of the mass transfer coefficients of various dense layers (dashed lines) of PTMSP, Teflon AF2400 or PMP of porous PVDF membranes (solid line). The km of the PVDF support (5.6 10^{-2} ms^{-1} for a thickness of 200µm) was calculated from our experimental data and the km of the dense layers from literature data (see Table 1S in DIB).

Moreover, this simple approach based on the prediction of the mass transfer coefficient demonstrates that the idea of using a dense layer to design a composite membrane definitively

resistant to wetting is compatible with reasonable water productivity and can fulfill industrial requirements. Indeed, with Teflon AF or PTMSP as coating layers and PVDF as the supporting layer, the water productivity is increased a lot when the thickness is below 1 µm. When the thickness of the coating layer is as thin as 0.1 µm, the water productivity can reach 38% to 63% of the pristine PVDF membrane. Today, this thickness value of 0.1µm can be readily achieved with industrial coating facilities.

Following the above approach, it was decided to prepare several composite membranes based on the prediction model and on the intrinsic properties of the polymers. The commercial microfiltration membrane PVDF was used as a porous support, and three hydrophobic polymers were tested as a dense layer, namely, polymethylpentene (PMP), poly(1-trimethylsilyl-1-propyne) PTMSP, and Teflon AF®2400, because these polymers have significant free volume and good thermal resistance.

3.3.1 Scanning electronic microscopy (SEM) observation of the composite membranes

Table 1 shows the morphology of pristine PVDF and three composite membranes with coatings of PMP, TeflonAF 2400 and PTMSP. Pristine PVDF is a porous structure with irregular macrovoids, and the structures of the top and bottom surfaces are similar [42]. The section views of composite membranes PMP, PTMSP, and AF2400 clearly indicate that the dense layer does not seem to enter into the porous structure of PVDF. As expected, the bottom sides keep the same initial structure of pristine PVDF.

Table 1: SEM images for pristine PVDF and composite hydrophobic membranes

Membrane	Dense layer (±1 µm)	Cross section	Top	Bottom
PVDF pristine	-	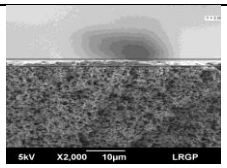	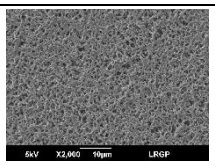	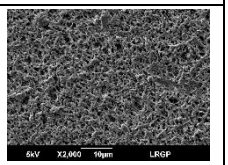
AF2400	~2	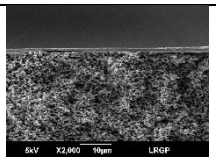	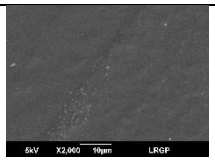	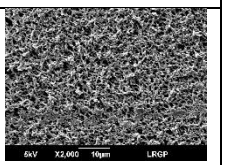
PMP	~15	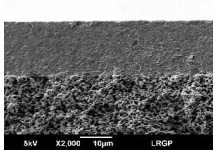	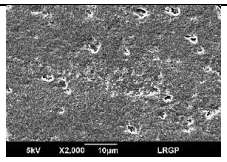	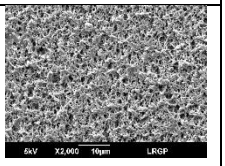

PTMSP	~5	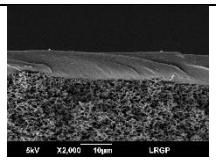	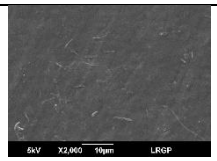	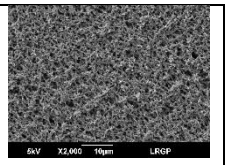

3.3.2 Contact angle measurements

The contact angle provides information about the affinity between a liquid and a surface, i.e., a high angle means a low affinity. With porous membranes, such as in conventional MD, to prevent the intrusion of water into the pores, the surface must be hydrophobic to avoid any spontaneous pore wetting. The contact angle determines the value of the liquid entry pressure in the case for porous membrane [43]. In the case of composite membranes, if the top surface of the pristine PVDF is coated totally by a dense layer the contact angle must be different and close to the contact angle of the polymer used for coating. The measured values of the top surfaces of our membranes are given in **Table 2** and a similar value was found in the literature for each polymer. This means that the surface is coated by the new polymer.

Table 2: Contact angle of pristine PVDF and composite membranes.

Membrane	Contact angle (°) this work	Contact angle (°) Literature	Reference
PMP	96	98	[44]
PTMSP	83	88	[45]
AF2400	112	105	[46]
Pristine PVDF	126	127	[42]

Details of the measurements are given in the supplementary **Table 2S**.

3.3.3 Studies of the mechanical stability of the composite membranes via adhesion tests

The adhesion test was carried out to check the mechanical stability of the active layer. The results are represented in **Figure 6**. Each test shows that under the pulling stress, breaking

is observed at the PVDF support level or glue level. These results indicate that the adhesion is very good between the support and the-coated hydrophobic layer. Data are given in the supplementary **Table 3S**.

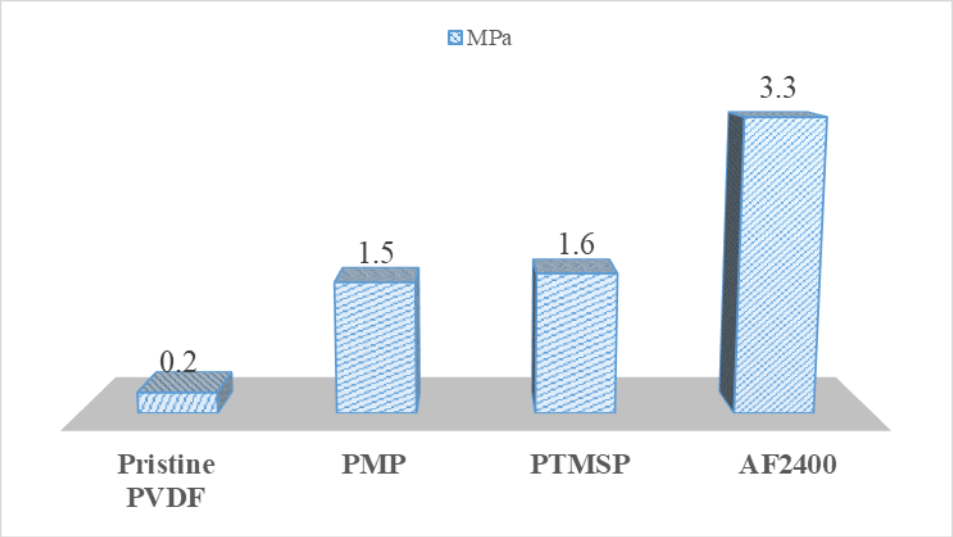

Figure 6: Mean results of pull-off adhesion tests of the composite membranes comparatively to the pristine PVDF membrane.

3.3.4 Fourier transform infrared spectrometry (FTIR) characterization

The FTIR spectra of pristine PVDF and the three composite membranes are shown in **Figure 7.** For each composite membrane, characteristic peaks of the coating polymer could be identified. The PVDF+PTMSP membrane shows a peak near 800 cm^{-1} that is assigned to the stretching of the -Si-CH3 group. The PVDF+PMP spectrum shows peaks in the range 3000-2950, which were attributed to -CH stretching in CH_3. PVDF +AF2400 is characterized by its CF3 peak close to 1200 cm^{-1}. The FTIR analyses confirm the modification surface of the PVDF support, and the observed characteristic peaks matched well with the literature data [47–49].

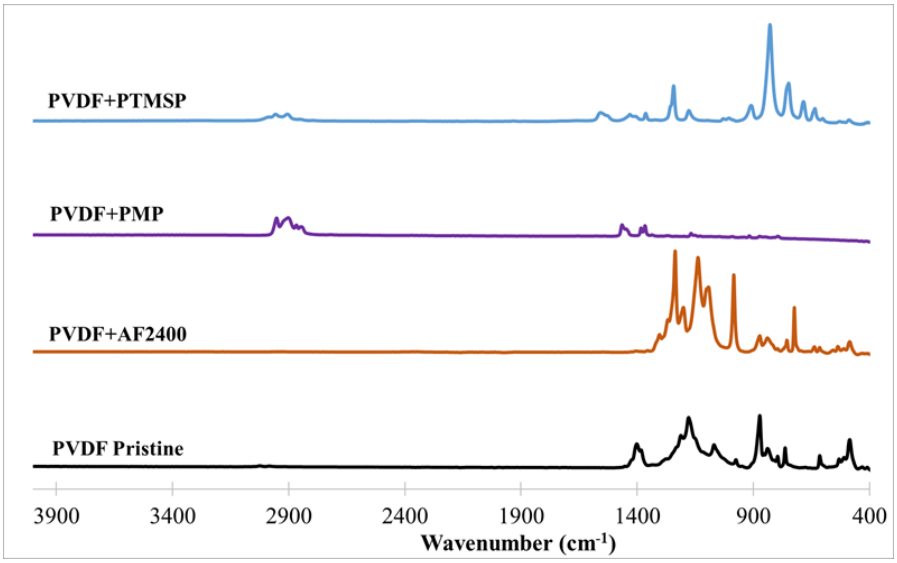

Figure 7: FTIR of pristine PVDF and composite membranes.

3.4 Desalination experiments

3.4.1 Blank experiment: case of pure water permeation

All experiments were carried out with a direct contact membrane cell (DCM) used for porous and dense composite membranes by using pure water in the feed and in the permeate sides of the membrane, with a duration of several hours. The stability of the temperature on the cold and hot sides of the membrane cell test was carefully controlled to ensure constant driving force and transmembrane fluxes (**Figure 3S**, Supplementary material section). As shown in **Figure 8**, the temperature difference and the measured partial pressure difference were both constant throughout the experiment with the setup.

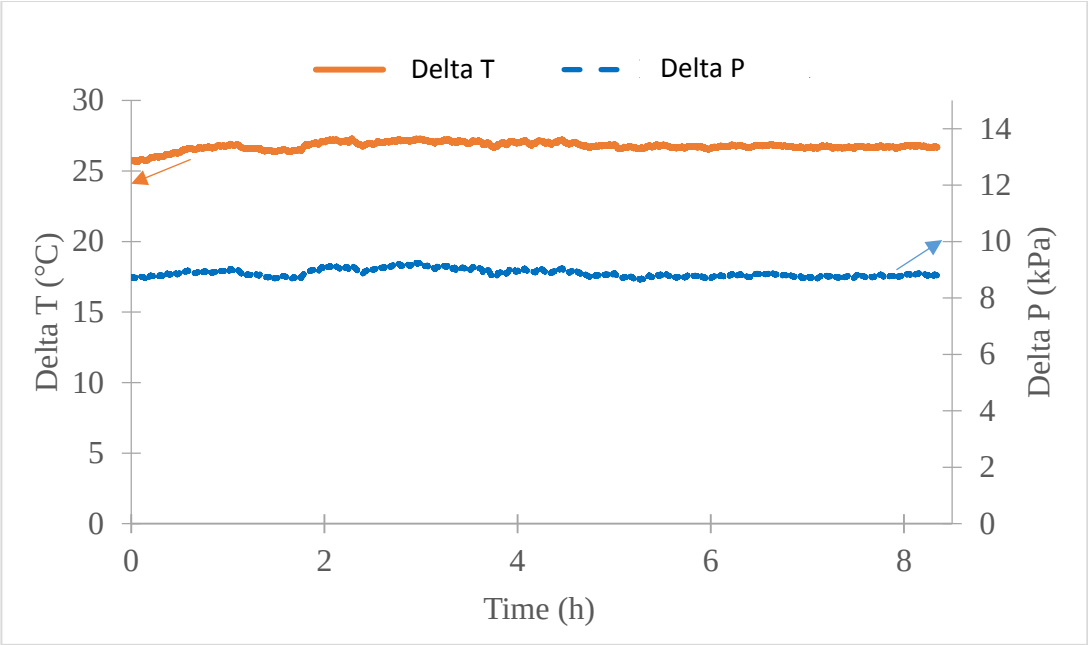

***Figure 8**: Example of the stability of the applied temperatures and driving force* versus *time. Case of PVDF+AF2400 with pure water. Temperature difference: solid line; pressure difference: dashed line.*

Analogous experiments were carried out with pristine, porous PVDF and composite membranes. For each membrane, the measured water flux was found to be effectively constant from the start of the steady state period to the end of the test at 8.5 hours (Supplementary material **Figure** 4S, 5S). These data confirm the good stability of the direct contact membrane cell setup for hours.

All the water permeance results are gathered in Figure 9; it can be seen that the porous PVDF membrane could give rise to a permeance of about 250 $kg.m^{-2}.h^{-1}.bar^{-1}$, while the composite membranes with dense layer of AF2400 and PTMSP reached permeance of 30 and 25 $kg.m^{-2}.h^{-1}.bar^{-1}$, respectively. For the third composite membrane prepared with PMP, a lower permeance of 5 $kg.m^{-2}.\ h^{-1}.bar^{-1}$ was obtained as expected, because of the higher thickness of the dense top layer, i.e., 15 µm.

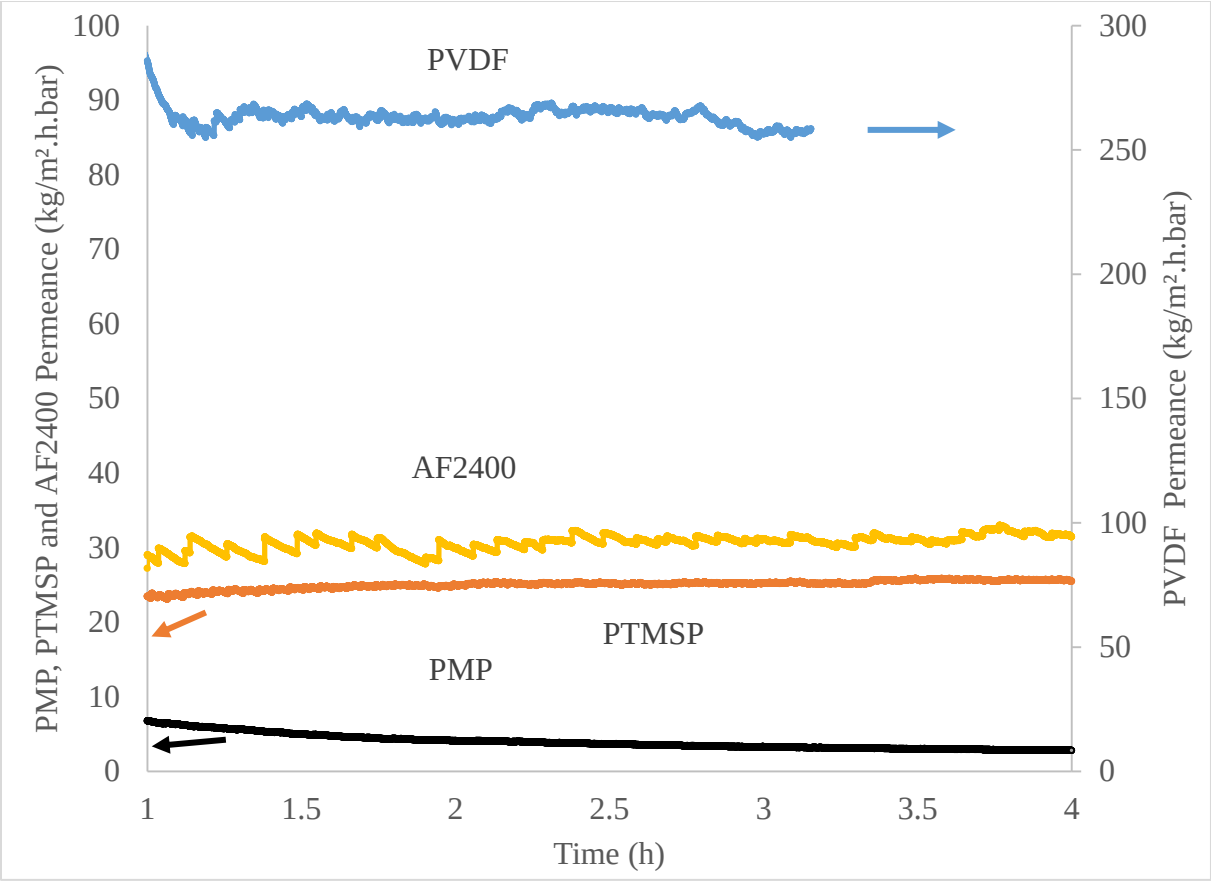

Figure 9: Permeance of pure water versus *time for porous PVDF and composite membranes.*

At first glance, the difference between the permeance of the pristine PVDF and of the composite membranes can seem substantial because they reach only 10% of the PVDF permeance. Nevertheless, it is worth noting that these homemade membranes are far from being optimized from the viewpoint of the thickness of the top layer. Indeed, it is known that industrial procedures now allow the coating of much thinner, defect-free top layers in the range of 0.1-1 micrometer. Hence, considering the resistance-in-series model (cf. Figure 5), the intrinsic mass transfer resistance of optimized composite membrane should be reduced to a large extent by reducing the top layer thickness. The simulation of the mass transfer coefficient and permeance of such composite membranes can be easily calculated (Equation 1); they are given in **Table 3** for a thickness of 0.1µm the top layer. As the mass transfer coefficient varies as $1/(R_{support}+R_{top\_layer})$, the permeance rapidly increases when the thickness of the top layer is decreased, clearly showing that much higher permeance should be obtained with the composite membranes.

Table 3: Calculation of the mass transfer coefficients and of the water permeance of the composite membranes using the experimental PVDF support permeance and the permeability of the dense top layer of PTMSP or Teflon AF2400.

	Support	**Prediction for composite membranes** [b]	
	PVDF (122 µm)	**PTMSP** (0.1 µm)	**TeflonAF** (0.1 µm)
Mass transfer coefficient (m/s)	9.2E-02 [a]	4.8E-02	2.5E-02
Water Permeance (kg/(m^2.h.bar))	250	129	69

a) Calculated from the experimental data

b) Calculated according the equation (2), using the literature permeability data; the conversion factor permeability from in Barrer to (mol.m)/(m^2.s.Pa) is 3.34 10^{-16} .

The main conclusions of this first set of experiments with pure water are that stable composite membranes can be obtained and that the resistance-in-series model predicted promising results in terms of the water permeance with the top layer in the range of 0.1 µm and a PVDF support of 122µm. Indeed these composite membrane are expected to have rather permeation performances because no wetting phenomena can occur whereas porous distillation membranes are known for having a fast, dramatic decrease of their permeance.

3.4.2 Desalination experiments: performance and stability

Using similar conditions (feed temperature inlet 50°C and permeate temperature inlet 20°C), the above set of membranes were used to achieve the desalination of three aqueous solutions of NaCl: 3 g/L, 10 g/L and 10 g/L + 1 g/L of the surfactant SDS. As the conductimetry method used to control any leak of salt in the permeate is a very sensitive method, it was not necessary to used high salt concentration. In addition, using these relatively low salt concentrations helps to carry out the experiments with a high driving force both in PV and in MD.

For each experiment, the system was first operated with pure water to reach steady state conditions. Then, the composition of the feed was adjusted to the desired concentration and maintained until reaching the steady state. The main objective was to measure the salt rejection and to compare the results obtained with the pristine PVDF membrane and with the three lab-made pervaporation membranes (Teflon AF2400, PMP and PTMSP).

Figure 10 shows these results with the first feed solution (3 g/L). After an initial period of stabilization following the addition of the salt on the feed side, the permeance of each membrane was constant versus time. For the porous PVDF membrane, no indication of wetting was observed during the whole experiment, as expected under these conditions.

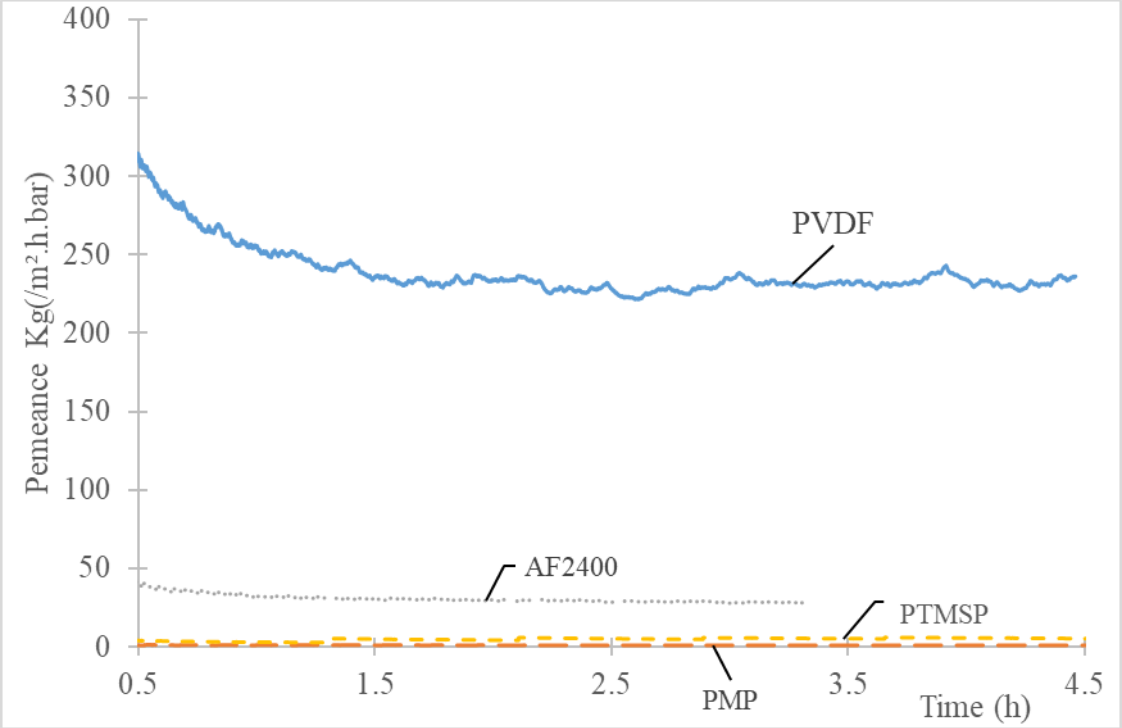

Figure 10: Desalination experiments. Permeance vs *time of the pristine PVDF (solid line) and of the composite membranes (dashed lines). Feed: 3 g/L NaCl, temperature difference: 30°C.*

The value of the conductivity of the water solution circulating downstream of the membrane was also monitored simultaneously. Compared to the value of the feed solution (6 mS/cm), the values of conductivity measured on the permeate side were steady and very small, in the range of 1.5 to 5 µS/cm, as shown in **Figure** 11. These values confirmed that under these operating conditions, no salt could cross the membranes, neither with the porous membrane nor with the dense composite ones.

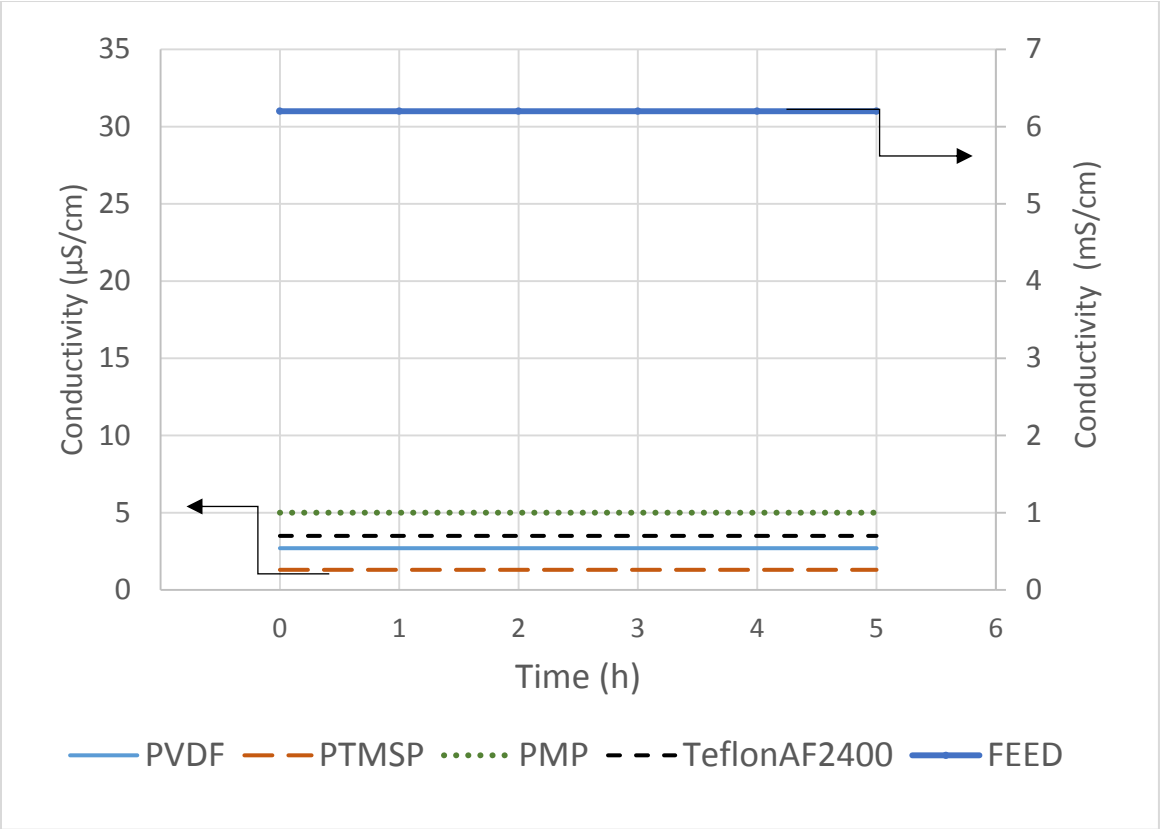

Figure 11: Monitoring of the permeate conductivity during the desalination experiments with PVDF (solid line) and the three composite membranes (dashed lines). The upper thick line shows the value of the conductivity on the feed side, 3 g/L. The salt concentration in the feed and initial conductivity are 3 g/L and 6 mS/cm, respectively. Temperature difference: 30°C.

3.4.3 Wetting resistance of the composite membranes

To evaluate the resistance of the membranes to the wetting phenomena, which is known to occur over time with porous distillation membranes, such as PVDF, the experiments were repeated under more drastic conditions, i.e., using a feed containing both a higher NaCl concentration and a surfactant, SDS at 1 g/L. SDS is a surfactant that is well known to induce a decrease in the surface tension of water solutions. Starting with pure water as the feed, the experiments were carried out with each membrane, and then the salt concentration of the feed was increased stepwise to 3 g/L and then to 10 g/L (Figure 12). For these two concentrations, the water permeance was almost steady for the three membranes (PVDF ≈ 300 $kg.h^{-1}.m^{-2}.bar^{-1}$ and PV membranes ≈ 3 $kg.h^{-1}.m^{-2}.bar^{-1}$). Especially the value of conductivity recorded for these three membranes was extremely small (<5 µS/cm) showing that no wetting phenomena occurred at this step.

After approximately 3 h, SDS was finally added to the feed as a water solution. The Figure 12 also gathered the results of the permeance (dashes lines) and of the conductivity (bold lines) obtained with these conditions on the right hand-side. It can be seen that almost immediately, the conductivity corresponding to the PVDF began dramatically to rise (factor 1000), while its permeance started to decrease significantly (slope ≈ -25 $kg.h^{-1}$, i.e., 8% loss). In contrast, no significant modification was observed for the PV membranes, neither for the permeance nor for the conductivity.

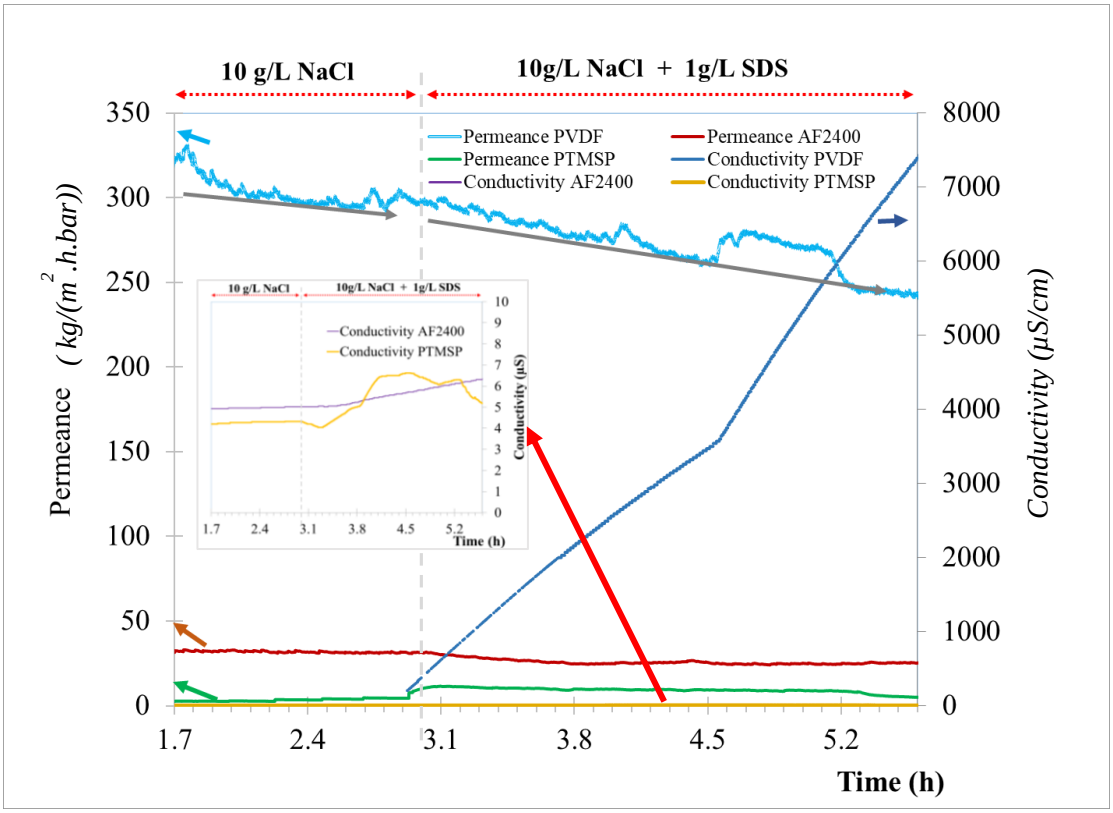

Figure 12: Investigation of the wetting resistance of the membranes versus feeds containing successive NaCl (up to 10 g/L) and NaCl with a surfactant (SDS 1 g/L). Permeance is given as dashed lines and the conductivity as solid lines. The black arrows indicate the negative slopes of PVDF permeance before and after the addition of SDS. Note also that the conductivity related to PTMSP and AF2400 are both very small and fused on the x axis, as shown by zooming.

These results clearly indicated that a part of the porous structure of the PVDF membrane became very rapidly wet, allowing NaCl to cross the membrane and increasing the mass transfer resistance for the water vapor. (**Figure** 6S, Supplementary material section). The transparent flat cell used in our setup allowed us to visualize the development of the wetting

phenomenon from the inlet to the outlet of the feed (**Figure** 7S, Supplementary material section).

4. Conclusion

The results presented in this work allow us to draw very positive conclusions on the potential industrial use of pervaporation membranes for water treatment applications such as desalination. Indeed, a very important challenge in desalination is to be able to design and prepare membranes that can withstand the wetting phenomenon, which currently precludes porous membranes from being used in membrane distillation. Confirming previous results, this work provides evidence that pervaporation can totally prevent wetting, even in the presence of surfactant in the feed.

Moreover, these results show that hydrophobic composite membranes that have a top dense layer are very promising candidates to develop highly permeable membranes for water. Indeed, there is no need to use hydrophilic membranes, which could lose their stability over time due to the swelling phenomenon or partial dissolution in water feeds.

Using a simple predictive approach based on the resistance-in-series model, it was also shown that the dramatic decline of the permeance usually observed with pervaporation membranes could be avoided if the polymers used to prepare the selective top layer are adequately chosen to match with the porous support properties. The main parameters to be controlled are as follows:

- the polymer permeability together with the layer thickness to tune the permeance of the selective layer for water and to obtain composite membranes with a mass transfer coefficient quite close to the mass transfer coefficient of the conventional porous distillation membrane like PDVF.
- the compatibility of the polymer for the material used as porous support to ensure good adhesion between the networks and to avoid delamination hazards in water solutions.
- the surface properties of the porous support, which should prevent the intrusion of the coating polymer into the pores of the support.

It was shown that even glassy polymers, which cannot be swollen by water, are promising candidates. With thicknesses in the range of 0.1 to 1 µm, the permeability for water should be above 4000 Barrer.

This work made use of super glassy polymers, e.g., PTMSP, Teflon AF 2400 and PMP, but other polymers endowed with high free volumes, such as PIM, may also be good candidates. The obtained results also mean that such membranes may be useful for treating hypersaline solutions, such as brine, issued from the use of RO technology. Finally, it should also be emphasized that a further advantage of a pervaporation membrane using a polymeric top layer should be less prone to fouling than conventional MD membranes because the polymeric dense top layer has no physical pores.

Acknowledgments: This work was achieved within the framework of the collaborative project ANR WETTMEM n° **ANR-14-CE04-0008** (2014-2017). The authors are very grateful to *Région* ***GrandEst*** and to Europe, programme ERASMUS (**project EU-METALIC**), for their financial support and grant for Dr. T. Eljaddi.

References

[1] Global status report on water safety plans: A review of proactive risk assessment and risk management practices to ensure the safety of drinking-water, (n.d.). http://apps.who.int/iris/bitstream/10665/255649/1/WHO-FWC-WSH-17.03-eng.pdf?ua=1 (accessed July 10, 2017).

[2] H. El-Dessouky, H. Ettouney, F. Al-Juwayhel, H. Al-Fulaij, Analysis of Multistage Flash Desalination Flashing Chambers, Chem. Eng. Res. Des. 82 (2004) 967–978. https://doi.org/10.1205/0263876041580668.

[3] C. Qi, X. Wang, H. Feng, Q. Lv, Performance analysis of low-temperature multi-effect distillation system under different feeding modes, Appl. Therm. Eng. 112 (2017) 1452–1459. https://doi.org/10.1016/j.applthermaleng.2016.10.165.

[4] S. Burn, M. Hoang, D. Zarzo, F. Olewniak, E. Campos, B. Bolto, O. Barron, Desalination techniques — A review of the opportunities for desalination in agriculture, Desalination. 364 (2015) 2–16. https://doi.org/10.1016/j.desal.2015.01.041.

[5] N. Ghaffour, T.M. Missimer, G.L. Amy, Technical review and evaluation of the economics of water desalination: Current and future challenges for better water supply sustainability, Desalination. 309 (2013) 197–207. https://doi.org/10.1016/j.desal.2012.10.015.

[6] D.L. Shaffer, J.R. Werber, H. Jaramillo, S. Lin, M. Elimelech, Forward osmosis: Where are we now?, Desalination. 356 (2015) 271–284. https://doi.org/10.1016/j.desal.2014.10.031.

[7] Q. Wang, N. Li, B. Bolto, M. Hoang, Z. Xie, Desalination by pervaporation: A review, Desalination. 387 (2016) 46–60. https://doi.org/10.1016/j.desal.2016.02.036.

[8] S. Alobaidani, E. Curcio, F. Macedonio, G. Diprofio, H. Alhinai, E. Drioli, Potential of membrane distillation in seawater desalination: Thermal efficiency, sensitivity study and cost estimation, J. Memb. Sci. 323 (2008) 85–98. https://doi.org/10.1016/j.memsci.2008.06.006.

[9] H. Ramlow, R.K.M. Ferreira, C. Marangoni, R.A.F. Machado, Ceramic membranes applied to membrane distillation: A comprehensive review, Int. J. Appl. Ceram.

Technol. 16 (2019) 2161–2172. https://doi.org/10.1111/ijac.13301.

[10] C.Y. Pan, G.R. Xu, K. Xu, H.L. Zhao, Y.Q. Wu, H.C. Su, J.M. Xu, R. Das, Electrospun nanofibrous membranes in membrane distillation: Recent developments and future perspectives, Sep. Purif. Technol. 221 (2019) 44–63. https://doi.org/10.1016/j.seppur.2019.03.080.

[11] F. Yalcinkaya, A review on advanced nanofiber technology for membrane distillation, J. Eng. Fiber. Fabr. 14 (2019). https://doi.org/10.1177/1558925018824901.

[12] N. Ghaffour, S. Soukane, J.-G.G. Lee, Y. Kim, A. Alpatova, Membrane distillation hybrids for water production and energy efficiency enhancement: A critical review, Appl. Energy. 254 (2019) 113698. https://doi.org/10.1016/j.apenergy.2019.113698.

[13] L.N. Nthunya, L. Gutierrez, S. Derese, E.N. Nxumalo, A.R. Verliefde, B.B. Mamba, S.D. Mhlanga, A review of nanoparticle-enhanced membrane distillation membranes: membrane synthesis and applications in water treatment, J. Chem. Technol. Biotechnol. 94 (2019) 2757–2771. https://doi.org/10.1002/jctb.5977.

[14] M.S. El-Bourawi, Z. Ding, R. Ma, M. Khayet, A framework for better understanding membrane distillation separation process, J. Memb. Sci. 285 (2006) 4–29. https://doi.org/10.1016/j.memsci.2006.08.002.

[15] K.J. Lu, Y. Chen, T.S. Chung, Design of omniphobic interfaces for membrane distillation – A review, Water Res. 162 (2019) 64–77. https://doi.org/10.1016/j.watres.2019.06.056.

[16] N.G.P. Chew, S. Zhao, R. Wang, Recent advances in membrane development for treating surfactant- and oil-containing feed streams via membrane distillation, Adv. Colloid Interface Sci. 273 (2019) 102022. https://doi.org/10.1016/j.cis.2019.102022.

[17] M.R. Choudhury, N. Anwar, D. Jassby, M.S. Rahaman, Fouling and wetting in the membrane distillation driven wastewater reclamation process – A review, Adv. Colloid Interface Sci. 269 (2019) 370–399. https://doi.org/10.1016/j.cis.2019.04.008.

[18] G. Naidu, S. Jeong, S. Vigneswaran, T.M. Hwang, Y.J. Choi, S.H. Kim, A review on fouling of membrane distillation, Desalin. Water Treat. 57 (2016) 10052–10076. https://doi.org/10.1080/19443994.2015.1040271.

[19] E. Korngold, E. Korin, I. Ladizhensky, Water desalination by pervaporation with

hollow fiber membranes, Desalination. 107 (1996) 121–129. https://doi.org/10.1016/S0011-9164(96)00157-9.

[20] H.B. Al-Saffar, B. Ozturk, R. Hughes, A comparison of porous and non-porous gas-liquid membrane contactors for gas separation, Chem. Eng. Res. Des. 75 (1997) 685–692. https://doi.org/10.1205/026387697524182.

[21] J.G. Wijmans, R.W. Baker, The solution-diffusion model: a review J.G., J. Memb. Sci. 107 (1995) 1–21. https://doi.org/10.1016/S0166-4115(08)60038-2.

[22] R. Bagger-Jørgensen, A.S. Meyer, M. Pinelo, C. Varming, G. Jonsson, Recovery of volatile fruit juice aroma compounds by membrane technology: Sweeping gas versus vacuum membrane distillation, Innov. Food Sci. Emerg. Technol. 12 (2011) 388–397. https://doi.org/10.1016/j.ifset.2011.02.005.

[23] M. Naim, M. Elewa, A. El-Shafei, A. Moneer, Desalination of simulated seawater by purge-air pervaporation using an innovative fabricated membrane, Water Sci. Technol. 72 (2015) 785–793. https://doi.org/10.2166/wst.2015.277.

[24] W. Zhong, Q. Li, X. Zhao, S. Chen, Membrane Preparation for Unconventional Desalination by Membrane Distillation and Pervaporation, in: Springer, Cham, 2020: pp. 265–293. https://doi.org/10.1007/978-3-030-33978-4_7.

[25] J.-P. Mericq, S. Laborie, C. Cabassud, Vacuum membrane distillation of seawater reverse osmosis brines, Water Res. 44 (2010) 5260–5273. https://doi.org/10.1016/j.watres.2010.06.052.

[26] I.L. Borisov, V. V. Volkov, Thermopervaporation concept for biobutanol recovery: The effect of process parameters, Sep. Purif. Technol. 146 (2015) 33–41. https://doi.org/10.1016/j.seppur.2015.03.023.

[27] P. Aptel, N. Challard, J. Cuny, J. Neel, Application of the pervaporation process to separate azeotropic mixtures, J. Memb. Sci. 1 (1976) 271–287. https://doi.org/10.1016/S0376-7388(00)82272-3.

[28] J.B. Xu, D.A. Spittler, J.P. Bartley, R.A. Johnson, Alginic acid-silica hydrogel coatings for the protection of osmotic distillation membranes against wet-out by surface-active agents, J. Memb. Sci. 260 (2005) 19–25. https://doi.org/10.1016/j.memsci.2005.03.017.

[29] J.B. Xu, J.P. Bartley, R.A. Johnson, Preparation and characterization of alginate-

carrageenan hydrogel films crosslinked using a water-soluble carbodiimide (WSC), J. Memb. Sci. 218 (2003) 131–146. https://doi.org/10.1016/S0376-7388(03)00165-0.

[30] A. Chanachai, K. Meksup, R. Jiraratananon, Coating of hydrophobic hollow fiber PVDF membrane with chitosan for protection against wetting and flavor loss in osmotic distillation process, Sep. Purif. Technol. 72 (2010) 217–224. https://doi.org/10.1016/j.seppur.2010.02.014.

[31] C.M. Bell, Comparison of polyelectrolyte coated PVDF membranes in thermopervaporation with porous hydrophobic membranes in membrane distillation using plate-and-frame modules, Chem. Eng. Process. Process Intensif. 104 (2016) 58–65. https://doi.org/10.1016/j.cep.2016.02.013.

[32] W. Kaminski, J. Marszalek, E. Tomczak, Water desalination by pervaporation – Comparison of energy consumption, Desalination. 433 (2018) 89–93. https://doi.org/10.1016/j.desal.2018.01.014.

[33] L. Li, J. Hou, Y. Ye, J. Mansouri, V. Chen, Composite PVA/PVDF pervaporation membrane for concentrated brine desalination: Salt rejection, membrane fouling and defect control, Desalination. 422 (2017) 49–58. https://doi.org/10.1016/j.desal.2017.08.011.

[34] V. Gekas, C. Gonzalez, A. Sereno, A. Chiralt, F. Fito, Mass transfer properties of osmotic solutions. I. Water activity and osmotic pressure, Int. J. Food Prop. 1 (1998) 95–112. https://doi.org/10.1080/10942919809524570.

[35] J. Chirife, S.L. Resnik, Unsaturated Solutions of Sodium Chloride as Reference Sources of Water Activity at Various Temperatures, J. Food Sci. 49 (1984) 1486–1488. https://doi.org/10.1111/j.1365-2621.1984.tb12827.x.

[36] A. Riddick, W. B. Bunger, T.K. Sakano, Organic Solvents: physical properties and methods of purification. 4th ed. Series: Techniques of Chemistry, Volume 2. Wiley (New york).

[37] M. Kattula, K. Ponnuru, L. Zhu, W. Jia, H. Lin, E.P. Furlani, Designing ultrathin film composite membranes: The impact of a gutter layer, Sci. Rep. 5 (2015) 1–9. https://doi.org/10.1038/srep15016.

[38] A.J. Ashworth, Relation between gas permselectivity and permeability in a bilayer

composite membrane, J. Memb. Sci. 71 (1992) 169–173. https://doi.org/10.1016/0376-7388(92)85016-C.

[39] C. Makhloufi, E. Lasseuguette, J.C. Remigy, B. Belaissaoui, D. Roizard, E. Favre, Ammonia based CO2capture process using hollow fiber membrane contactors, J. Memb. Sci. 455 (2014) 236–246. https://doi.org/10.1016/j.memsci.2013.12.063.

[40] Y. Okamoto, J.H. Lienhard, How RO membrane permeability and other performance factors affect process cost and energy use: A review, Desalination. 470 (2019) 114064. https://doi.org/10.1016/j.desal.2019.07.004.

[41] B. Shi, P. Marchetti, D. Peshev, S. Zhang, A.G. Livingston, Will ultra-high permeance membranes lead to ultra-efficient processes? Challenges for molecular separations in liquid systems, J. Memb. Sci. 525 (2017) 35–47. https://doi.org/10.1016/j.memsci.2016.10.014.

[42] Y. Chen, M. Tian, X. Li, Y. Wang, A.K. An, J. Fang, T. He, Anti-wetting behavior of negatively charged superhydrophobic PVDF membranes in direct contact membrane distillation of emulsified wastewaters, J. Memb. Sci. (2017). https://doi.org/10.1016/j.memsci.2017.04.040.

[43] L. Eykens, K. De Sitter, C. Dotremont, L. Pinoy, B. Van der Bruggen, Membrane synthesis for membrane distillation: A review, Sep. Purif. Technol. 182 (2017) 36–51. https://doi.org/10.1016/j.seppur.2017.03.035.

[44] L. Shao, J. Samseth, M.B. Hagg, Effect of plasma treatment on the gas permeability of poly(4-methyl-2-pentyne) membranes, Plasma Process. Polym. 4 (2007) 823–831. https://doi.org/10.1002/ppap.200600219.

[45] A. V. Volkov, S.E. Tsarkov, A.B. Gilman, V.S. Khotimsky, V.I. Roldughin, V. V. Volkov, Surface modification of PTMSP membranes by plasma treatment: Asymmetry of transport in organic solvent nanofiltration, Adv. Colloid Interface Sci. 222 (2015) 716–727. https://doi.org/10.1016/j.cis.2014.11.005.

[46] J. Gomez, A.M.; Fraser-reid, B.; Cristobal Lopez, Fluorous chemistry, Springer, 2010.

[47] A. Khosravi, A. Vatani, T. Mohammadi, Application of polyhedral oligomeric silsesquioxane to the stabilization and performance enhancement of poly(4-methyl-2-pentyne) nanocomposite membranes for natural gas conditioning, J. Appl. Polym. Sci.

134 (2017) 19–23. https://doi.org/10.1002/app.45158.

[48] A. Limcharoen, P. Limsuwan, C. Pakpum, K. Siangchaew, Characterisation of C-F polymer film formation on the air-bearing surface etched sidewall of fluorine-based plasma interacting with AL2O 3-TiC substrate, J. Nanomater. 2013 (2013). https://doi.org/10.1155/2013/851489.

[49] K. Yamauchi, Y. Yao, T. Ochiai, M. Sakai, Y. Kubota, G. Yamauchi, Antibacterial activity of hydrophobic composite materials containing a visible-light-sensitive photocatalyst, J. Nanotechnol. (2011). https://doi.org/10.1155/2011/380979.

[50] A.A.-H. Al-Anezi, A.O. Sharif, M.I. Sanduk, A.R. Khan, Experimental Investigation of Heat and Mass Transfer in Tubular Membrane Distillation Module for Desalination, ISRN Chem. Eng. 2012 (2012) 1–8. https://doi.org/10.5402/2012/738731.